University of Groningen

In situ transmission electron microscopy study of the crystallization of Ge2Sb2Te5

Kooi, B. J.; Groot, W. M. G.; De Hosson, J. Th. M.

IMPORTANT NOTE: You are advised to consult the publisher's version (publisher's PDF) if you wish to cite from it. Please check the document version below.

Document Version
Publisher's PDF, also known as Version of record

Publication date:
2004

Link to publication in University of Groningen/UMCG research database

In situ transmission electron microscopy study of the crystallization of Ge$_2$Sb$_2$Te$_5$

B. J. Kooi,[a] W. M. G. Groot, and J. Th. M. De Hosson
Department of Applied Physics, Materials Science Centre and Netherlands Institute for Metals Research, University of Groningen, Nijenborgh 4, 9747 AG Groningen, The Netherlands

Crystallization of amorphous Ge$_2$Sb$_2$Te$_5$ films (10, 40, and 70 nm thick) was studied by *in situ* heating in a transmission electron microscope (TEM). Electron irradiation-induced crystallization is possible at room temperature using a 400 kV electron beam where the reciprocal of the incubation time for crystallization scales linearly with the current density during electron irradiation. Without electron-beam exposure, crystallization starts at 130 °C. Using a 200 kV beam, crystallization also occurred in the temperature interval between 70 and 130 °C. In principle, electron irradiation always affects the crystallization kinetics, strongly promoting nucleation and probably not hampering growth. At 130 °C without electron-beam exposure, 400 nm diameter colonies of 10–20 nm grains develop in the 40 and 70 nm thick films showing clear symmetric bending contour contrast. These spherulites prefer to have in their center the $\langle 111 \rangle$ zone axis of the Fm$\bar{3}$m structure perpendicular to the surface of the film and show a typical tilt variation of $\pm 10°$. At 340 °C, the transition from the metastable to the stable trigonal (P$\bar{3}$m1) crystal structure takes place. Fast and excessive grain growth occurs with the [0001] axis perpendicular to the film surface of the film. Also shown is that oxidation of the Ge$_2$Sb$_2$Te$_5$ film strongly influences its crystallization; its critical temperature decreases from 130 to 35 °C. © *2004 American Institute of Physics.* [DOI: 10.1063/1.1636259]

I. INTRODUCTION

In phase change optical recording, Ge$_2$Sb$_2$Te$_5$ is currently most widely used as the active medium for rewritable information storage.[1–4] Amorphous areas, embedded in a crystalline surrounding, act as bits of information. A relatively high laser power is used to write these amorphous spots and medium, and low laser powers are used for erasing (crystallization) and reading, respectively.

For the characterization of the functional physical properties of Ge$_2$Sb$_2$Te$_5$, e.g., the optical and electrical properties (e.g. see Refs. 4–9), most research in this growing field is performed using lasers. As a matter of course, a structural analysis is also performed, mainly using x-ray diffraction.[10,11] In contrast, transmission electron microscopy (TEM) is a more appropriate method to analyze, on a local scale, the structural changes involved in the crystallization process in Ge$_2$Sb$_2$Te$_5$.[5,12–15] TEM becomes particularly powerful if the crystallization process can be followed *in situ* in the microscope. Nevertheless, a disadvantage of TEM is that due to the thin sample needed, *in situ* studies of phase transformations are often not representative of the transitions occurring in the bulk. However, in the present context, TEM is ideal because the thickness of the Ge$_2$Sb$_2$Te$_5$ films used in practice is already optimal for TEM study. Thus far one extensive *in situ* TEM study has been reported in literature.[15] It was used to analyze in detail the kinetics of the amorphous to crystalline phase transformation in terms of the Johnson–Mehl–Avrami–Kolmogorov formalism. However, informa-

tion on the structure and morphology of the films after crystallization is not presented. Moreover, any influence of the electron beam on the crystallization process was reported as being insignificant. In this article, we indicate that this is remarkable and we will show considerable differences in morphology and kinetics of the crystallized film inside and outside the electron-beam exposed areas and will show that, in principle, the electron beam always affects the crystallization process. In addition, we have concentrated on the transformation from the metastable to the stable crystal structure. Finally, the strong effect of oxidation of the Ge$_2$Sb$_2$Te$_5$ film on the crystallization behavior is examined.

II. EXPERIMENT

Ge$_2$Sb$_2$Te$_5$ master alloys were produced by mixing the pure components (Ge:6N, Sb, and Te both 5N) in an evacuated quartz tube at 750 °C. After cooling down, it was checked using energy dispersive spectrometry (EDS) in a scanning electron microscope that the composition was sufficiently homogeneous across the whole ingot. No concentration gradients were detected. Pieces of the ingot were positioned in pockets for electron-beam evaporation. As substrates, 10 nm thick Si-nitride membranes were used. These transparent substrates were obtained by etching 100 $\times$ 100 μm^2 windows in a Si wafer containing a thin Si-nitride film on one side. A Varian electron-beam evaporator with a thickness monitor was used for the deposition of 10, 40, and 70 nm thick amorphous Ge$_2$Sb$_2$Te$_5$ films. The thickness monitor was based on pure Te and, therefore, the actual film thickness will be systematically slightly larger. Specimens were stored in a vacuum to prevent oxidation of the

---
[a]Author to whom correspondence should be addressed; electronic mail: b.j.kooi@phys.rug.nl

$Ge_2Sb_2Te_5$ film. Some films were capped with a continuous carbon film (10–20 nm thickness) using an Edwards resistance-heating evaporator.

For TEM, a JEOL 2010F operating at 200 kV [equipped with an energy dispersive x-ray spectrometry (EDS) detector and a Gatan Imaging Filter (GIF)] was used. A Gatan double tilt heating holder (model 652 with a model 901 SmartSet Hot Stage Controller) was used that employs a proportional integral differential controller for accurately controlling of the temperature (within $\pm 1\,°C$) and for a fast ramp rate to attain the desired final temperature without overshoot. A disadvantage of the temperature control is that the thermocouple is connected to the furnace at the edge of the sample. In the electron-transparent area in the center of the sample, the actual temperature is lower than that measured by the thermocouple. The higher the temperature, the larger the discrepancy between the actual and the displayed temperature. Also the poorer the thermal conductivity of the sample, the larger the time delay between the moment the temperature is reached at the edge and in the center of the sample. Therefore, we always analyzed the outer few microns of Si-nitride window where it connects to the thicker Si wafer. Images were recorded on a Gatan dual-view 300 W charge coupled device camera and on the Gatan multiscan camera that is part of the GIF. Because the electron beam of the TEM can influence the crystallization process, we either imaged the sample at elevated temperature, but in areas that were not previously exposed to electrons, or we cooled down and imaged at room temperature (after which we continued with heating). Apart from the *in situ* heating experiments in the JEOL 2010F, some experiments were also performed with a JEOL 4000EX/II operating at 400 kV.

III. RESULTS

In the temperature window between 70 and 125 °C crystallization of amorphous $Ge_2Sb_2Te_5$ was only observed when assisted by the (200 kV) electron beam. At 80 °C, a high current density is needed to induce crystallization as can be observed in Fig. 1, where the total current (3 nA) produced by a field-emission gun is focused in an area with a diameter of about 100 nm. Figure 1(a) shows a bright-field TEM (BF-TEM) image and Figs. 1(b) and 1(c) show high-resolution TEM (HRTEM) images of the crystals with a typical diameter of 5–10 nm after heating for 5 min at 80 °C. In Fig. 1(b), the crystals were already merged and Fig. 1(c) shows a crystal viewed along a cubic zone axis.

Figure 1 holds for a $Ge_2Sb_2Te_5$ film thickness of 10 nm, whereas the figures below hold for a thickness of 40 nm. Decreasing the current density by spreading the electron beam in steps to larger diameters on previously unexposed areas required higher temperatures to arrive at the formation of observable crystallites after 5 min. For instance, Fig. 2 shows a BF-TEM image where crystallization was observed after 5 min of heating at 90 °C when the beam was 400 nm wide and at 120 °C when the beam had a diameter of 1.8 μm. At 50 °C crystallization was not observed even with the beam focused in an area with a diameter of 20 nm. At 130 °C, crystallization also occurs outside the area irradiated
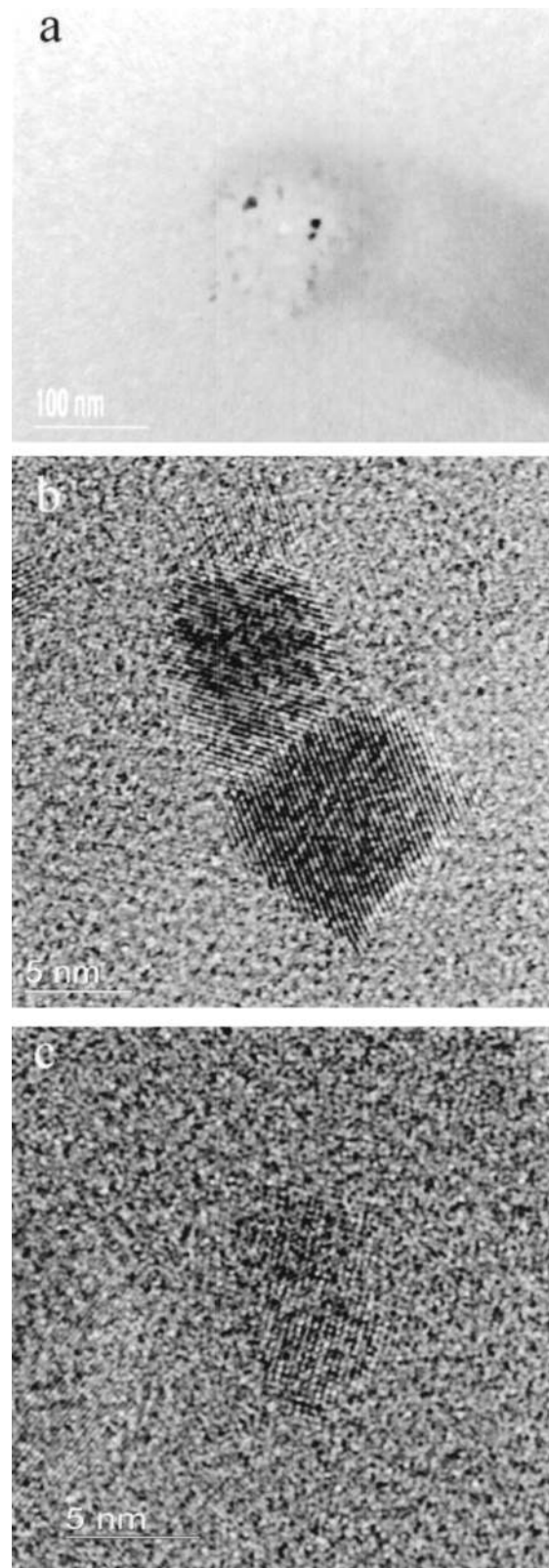
FIG. 1. (a) BF-TEM image showing electron-beam-induced crystallization of a 10 nm thick $Ge_2Sb_2Te_5$ film at 80 °C. (b) HRTEM image of a detail of (a) showing merging of 5–10 nm large crystals. (c) HRTEM image of a detail of (a) showing a nanocrystal viewed along its cubic zone axis.

by the electrons as can be seen in Fig. 3. Note the large difference in morphology and what at first sight appears as grain size of the crystals that were formed at 130 °C with and without electron irradiation. In the irradiated area, the typical
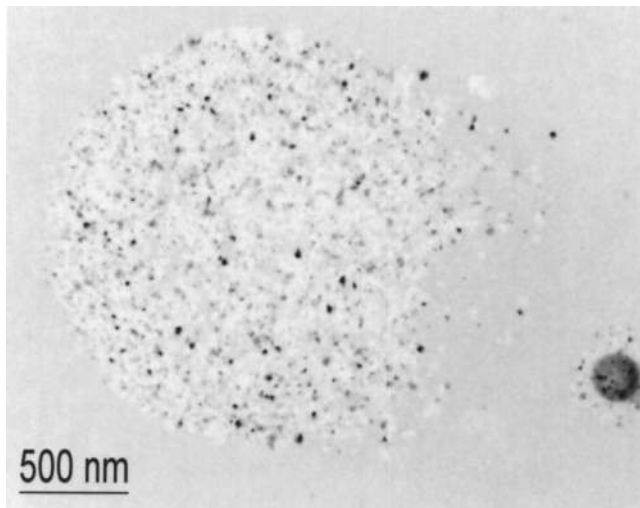
FIG. 2. BF-TEM image showing electron-beam assisted crystallization of a 40 nm thick $Ge_2Sb_2Te_5$ film after 5 min at 90 °C with an electron-beam diameter of 400 nm (area on the right-hand side) and after 5 min at 120 °C with an electron-beam diameter of 1.8 μm (area more or less in the center).

grain size is 10–20 nm and the grains have random orientations [as can be seen from selected area electron diffraction (SAED) patterns]. Outside this area, apparent large grains with a typical size of 400 nm are present. Closer inspection of these large grains reveals that they are in fact colonies
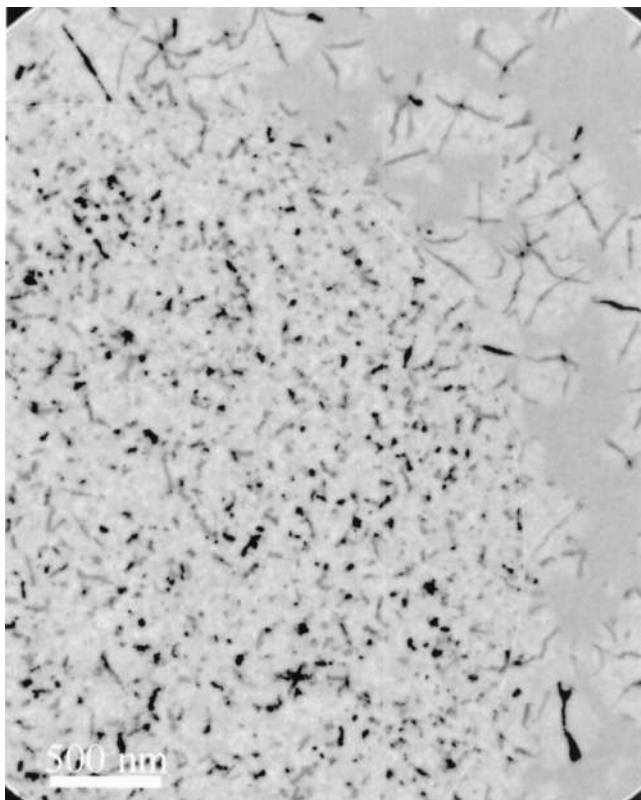

FIG. 3. BF-TEM image showing crystallization of a 40 nm thick $Ge_2Sb_2Te_5$ film after 5 min at 130 °C both *without* (top and right-hand side) and *with* electron-beam assistance (lower left-hand side). Note that only a part of the electron-irradiated with a diameter of 5.4 μm is shown and that the crystallization (both morphology and kinetics) is clearly different with and without electron-beam assistance.
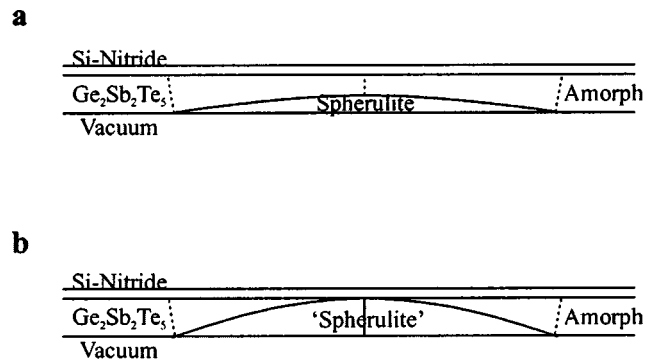

FIG. 4. Schematic representation of a crystalline colony developing in a 40 nm thick amorphous $Ge_2Sb_2Te_5$ film. The observed colonies, with typical width of 400 nm and tilt variation of $\pm 10°$, would correspond to a cap of a sphere with a diameter of 2.3 μm as shown in (a) or a cap of an ellipsoid with a size of 2.35 perpendicular to the film surface and a maximum diameter of 1.55 parallel to the film plane as shown in (b).

consisting of grains with a size of around 10 nm that have experienced cooperative growth. Most colonies show a symmetric pattern of black lines very similar to bend contours. Colonies with a three-fold symmetry (each 60°, a black line emerges from the center) are most abundant. These symmetries reveal the strong texture that is present within the colonies. If all grains within a colony would have identical orientation (i.e., as in a single crystal) then the contrast would be more or less uniform over a colony. Here, it is not. Tilting with only a few degrees shows that the symmetric black lines move across the colony like bending contours do. Because the Si-nitride substrate is flat this indicates that the grains in the center of the bend contour are exactly in a zone axis, but when moving to the periphery of the colony the grains start to tilt the zone axis in the radial direction. We observed that a tilt of typical 10° is present between the center and the edge of the colony having a typical size of 400 nm. This was checked by tilting in such a way that the center of the bend contour (present in the middle of a colony) was moved to the edge of the colony. On average, the larger the diameter of the observed colony in plan view, the larger the variation in tilt angle across the colony. The colonies thus strongly resemble spherulites.[16] However, note that the colony diameter is on average 400 nm compared to a thickness of 40 nm. In this way, a colony only corresponds to a thin cap of a sphere or ellipsoid as schematically shown in Fig. 4. A tilt variation of $\pm 10°$ across a colony with an observed width in plan view of 400 nm points at a sphere with a diameter of 2.3 μm as is shown in Fig. 4(a). Then, the height of the cap is about 18 nm, i.e., less than the film thickness of 40 nm. Using an ellipsoid, the height of the cap can be 40 nm, its width 400 nm, and the tilt variation $\pm 10°$ as is shown in Fig. 4(b). This ellipsoid has one long axis perpendicular to the plane of the film of 2.35 μm and a maximum diameter parallel to the film plane of 1.55 μm. Knowing on which side in the microscope the film/vacuum and the film/Si-nitride interface are present and observing to which (calibrated) side the center of the bend contour moves upon positive and negative tilt allows the distinction at which interface the spherulite nucleated. The results of these tilting experiments clearly demonstrate that nucleation occurs at the film/vacuum interface and not at

the film/Si-nitride interface. This result is also indicated in Fig. 4.

Spherulites were also observed in the 70 nm thick film where they tend to be slightly larger, but not in the 10 nm thick film. Apparently, and not surprisingly, a minimum film thickness is needed to enable the growth of the spherulites.

The different morphology of the crystallization inside and outside the irradiated area shows that the electron beam is particularly effective in creating nuclei for crystallization and is not assisting in the growth of the crystals since they keep a size of the order of 10–20 nm. In this sense, the crystallization is nucleation driven.[4] On the other hand, at 130 °C without irradiation, the number of nuclei formed as a function of time is still very low and these nuclei grow to relatively large colonies and in this sense the crystallization appears growth driven.[4] Using laser irradiation, it was observed that the crystallization in $Ge_2Sb_2Te_5$ films is nucleation driven and in this sense the process seems to resemble more the one aided by electron irradiation than by thermal activation alone.

After 5 min at 130 °C crystallization inside the irradiated area is completed. However, outside this area the crystallization is finalized when the temperature is raised up to 140 °C [see Fig. 5(a)]. Figure 5(b) shows an SAED pattern of the area indicated by the black circle in Fig. 5(a). The SAED pattern matches perfectly with a face-centered-cubic (fcc) crystal viewed along its ⟨111⟩ zone axis having a lattice constant of 0.60 ± 0.01 nm. This pattern corresponds well with the metastable NaCl-type structure of $Ge_2Sb_2Te_5$ having a lattice constant of 0.601 nm.[10,11] The diffraction pattern in Fig. 5(b) gives the impression that it originates from a single crystal. However, as explained above, this is not in accordance with the bend-contour contrast present in the colonies and with the tilting experiments. The positions of the spots in the pattern in Fig. 5(b) are not sensitive to tilt but the intensities of the spots are sensitive. If, however, the tilt occurs in a radial direction symmetric around the center of the bend contour and the center of this contour is more or less in the center of the selected area aperture, then the spot pattern will still have the appearance of a single crystal viewed perfectly along its zone axis.

Increasing the temperature above 140 °C does not lead to drastic changes, but increases the size of the individual crystallites in the colonies to typical 40–50 nm and results in void formation (cf. Fig. 6 that is recorded at 335 °C). The connected structure within the individual colonies is lost gradually during this anneal from 140 to 335 °C. Void formation has two origins: (1) Crystallization results in a denser structure due to the removal of free volume from the amorphous structure. This effect is expected to be small because, in the metastable NaCl-type crystal structure, 20% of vacancies are still present on one of the two fcc sublattices over which Ge and Sb are distributed (with Te occupying fully the other fcc sublattice). Nevertheless, a volume reduction of 6% has been reported when the metastable crystalline structure forms out of the amorphous one.[17] (2) Evaporation of the $Ge_2Sb_2Te_5$ film at the elevated temperatures. The images were recorded for films without a capping layer that are, of course, prone to evaporation in the vacuum of the TEM.
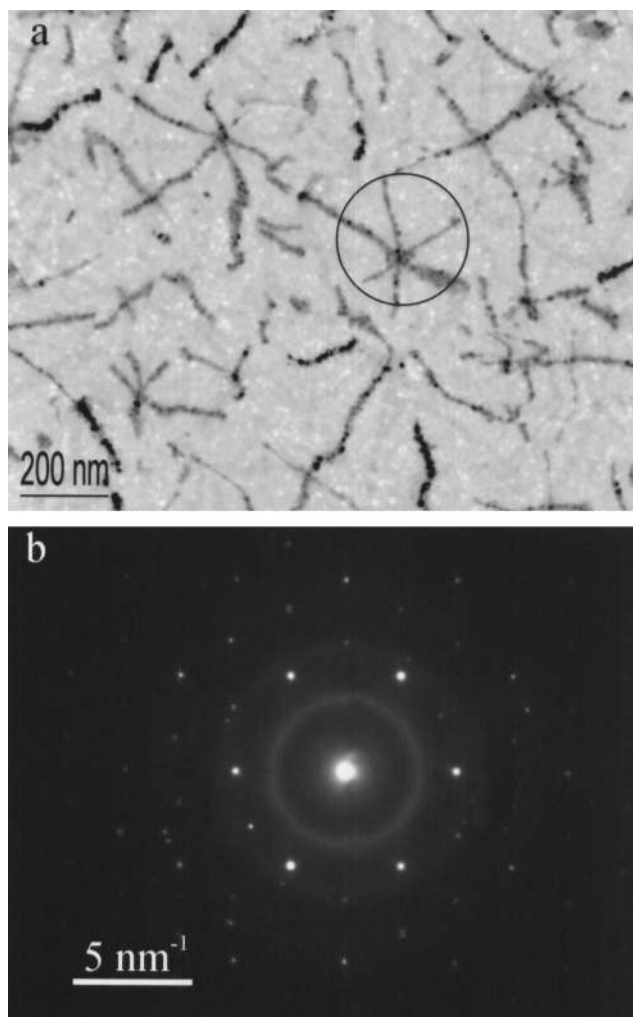

FIG. 5. (a) BF-TEM image showing a fully crystallized 40 nm thick $Ge_2Sb_2Te_5$ film after 5 min at 140 °C (without electron-beam assistance) showing crystals with bending-contour contrast. (b) SAED pattern of the circular area indicated in Fig. 4(a) showing a ⟨111⟩ zone-axis pattern of an fcc material having a lattice constant of 0.60 ± 0.01 nm.

Increasing the temperature to 340 °C results in a dramatic change. Excessive grain growth occurs where the grain boundary moves fast (of the order of a second) over many micrometers. Figure 7(a) shows a BF-TEM image with the corresponding SAED pattern in Fig. 7(b). Careful inspection of Fig. 7(b) shows that additional spots have appeared, as indicated by the arrows, compared to the ⟨111⟩ fcc zone axis pattern of Fig. 5(b). The pattern in Fig. 7(b) points at a hexagonal crystal structure viewed along its [0001] zone axis having a lattice constant $a = 0.424 \pm 0.007$ nm. This lattice constant corresponds well with the stable high-temperature crystal structure of $Ge_2Sb_2Te_5$ having a and c lattice constants of 0.425 nm and 1.727 nm, respectively.[18] Note that the voids with a triangular shape due to $\{11\bar{2}0\}$ facets (if these facets are observed edge on) that were rearranged very fast during the phase transformation. The [0001] texture in the film is very strong. Apparently, the basal planes in the trigonal structure want to be parallel to the surface or to the interface with the Si-nitride (the grains have a large aspect ratio and the influence of the grain-boundary energy is there-
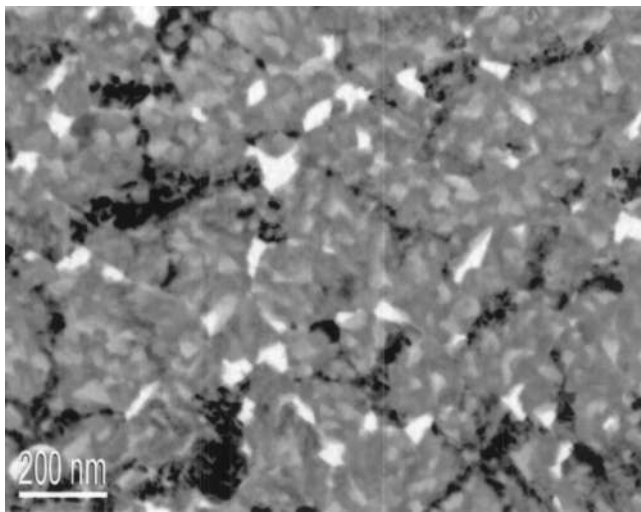
FIG. 6. BF-TEM image showing a crystallized $Ge_2Sb_2Te_5$ film after heating at 335 °C (without electron-beam assistance) showing coarsening of the crystallites that have to a large extent lost their connected structure in the colonies. Also voids develop.

fore negligibly small). Because each basal plane is only occupied by the atoms of one element, there may be a strong preference for a certain element at the surface in order to attain the lowest surface energy. It is known that thin films of amorphous Sb and Sb–Ge (with Sb>85 at. %) after crystallization develop a strong fiber texture with [0001] perpendicular to the surface.[19] Moreover, Sb is well known for its segregation tendency in many systems and for its behavior as a surfactant.[20] Therefore, it is quite likely that in the present system, Sb prefers to be the outermost atomic layer.

Oxidation of the $Ge_2Sb_2Te_5$ has a tremendous effect on the amorphous to crystalline transition temperature. After keeping a 10 nm thick $Ge_2Sb_2Te_5$ film for 2 weeks in air (in a conditioned room) heating was hardly necessary to crystallize the whole film; a temperature of 35 °C was sufficient as can be seen in Fig. 8. Notwithstanding the low-temperature crystallization occurred very fast (a matter of seconds for complete crystallization). Figure 8(a) shows an overview bright-field (BF) image and Fig. 8(b) a HRTEM image. The crystallites have a typical size of 40–50 nm and are strongly facetted. This is a totally different crystal morphology then the one observed after the normal crystallization at 130 °C (cf. Fig. 3). Grain boundaries give a distinct contrast; darker than the weakly diffracting crystalline grains and brighter than the grains showing a strong diffraction contrast [cf. Fig. 8(a)]. These grain boundaries still have an amorphous structure, probably due to the presence of amorphous Ge oxide. From the three elements present in the film, Ge has the highest oxygen affinity and is thus preferentially oxidized. The remaining film will thus become enriched in Sb and Te. It is known that the crystallization temperature (T_C) decreases as the relative amount of Sb_2Te_3 increases in the pseudo-binary GeTe-Sb_2Te_3 system; e.g., for GeTe a T_C of 170 °C is given,[21] for $Ge_2Sb_2Te_5 \sim 140$ °C[22,23] and for $Ge_1Sb_4Te_7$ ~ 120 °C.[22,23] Interesting in this context is that for Ge_xTe_{1-x} for x going from 0.2 to 0 the T_C decreases from about 200 to 0 °C.[21] Calculated values for the glass-transition temperature
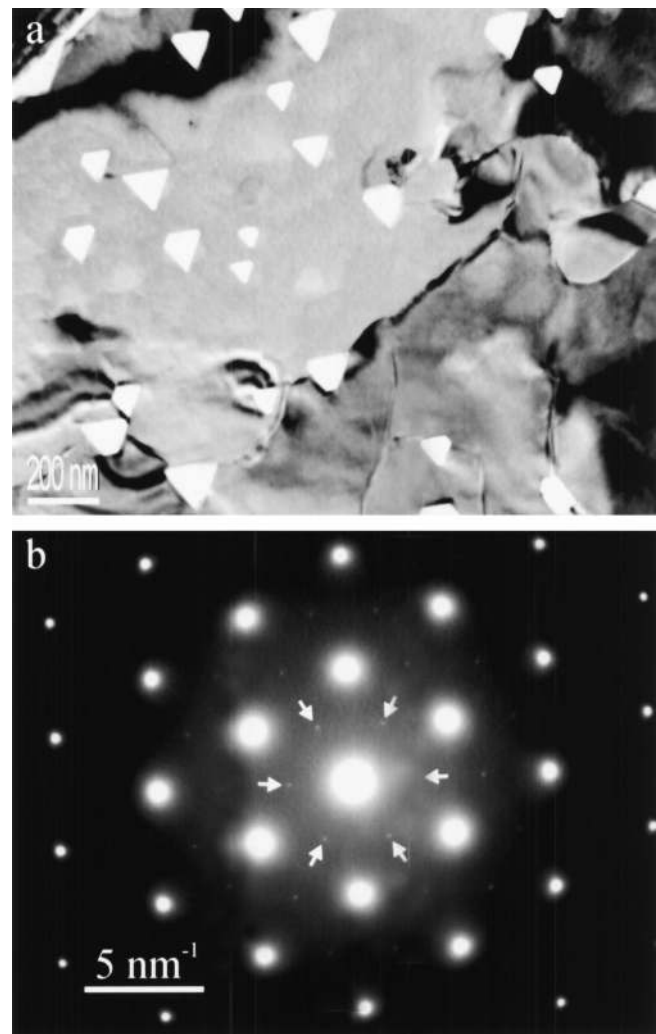

FIG. 7. (a) BF-TEM image showing the excessive grain growth that occurs at 340 °C when the metastable crystal structure transforms into the stable one. Voids with triangular shape develop in a single grain. (b) SAED pattern showing perpendicular to the surface an [0001] orientation of the $Ge_2Sb_2Te_5$ crystal, with $a = 0.424 \pm 0.007$ nm that points at the ($P\bar{3}$ m1) stable crystal structure. Arrows indicate the (weak) $\{10\bar{1}0\}$ reflections making the distinction between the stable and the metastable crystal structure [cf. Fig. 5(b)].

(T_g) for (all possible compositions in) the ternary Ge–Sb–Te system[23] show indeed that from $Ge_2Sb_2Te_5$ to "Sb_2Te_5" a decrease from 110 °C to about -10 °C occurs. Noting that T_C is always somewhat higher that T_g, the present finding fits well within this picture by a decrease from 130 to 35 °C.

All of our samples may have suffered weakly from oxidation, because they have to be transported through air to the TEM. However, the T_C of 130 °C we observed agrees well with what is generally found for $Ge_2Sb_2Te_5$. On the other hand, the sample kept 2 weeks in air shows a strong lowering of T_C. It is this distinct difference we want to present without a further detailed study of the effect of intermediate periods of exposure to air.

The temperature for the transition from the metastable to the stable crystal structure is not so strongly affected by oxidation. Now we find a temperature of 275 instead of 340 °C. Again, this transition is very distinct when it occurs within
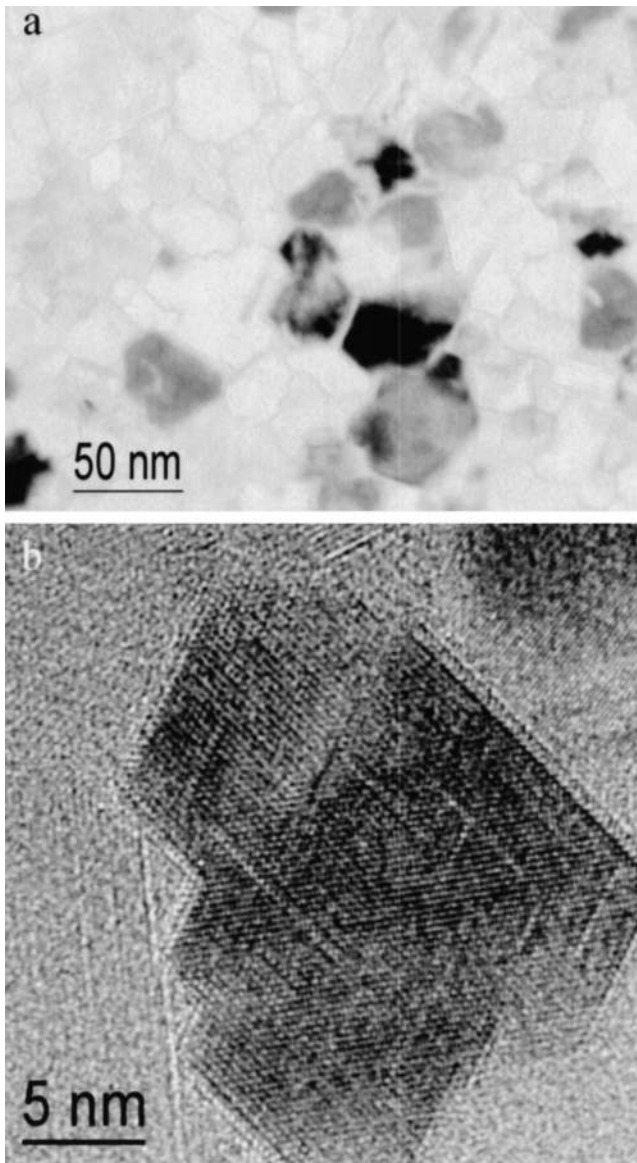
FIG. 8. (a) BF-TEM image showing the strong influence of the oxidation of a 10 nm thick $Ge_2Sb_2Te_5$ film resulting in crystallization at 35 instead of 130 °C and a totally different crystal morphology (cf. Fig. 3). The deviating contrast of the grain boundaries indicate the presence of an amorphous phase, possibly GeO_x leading to a Ge depleted alloy with totally different crystallization behavior. (b) HRTEM image showing a strongly facetted crystal surrounded by an amorphous phase.

the microscope. Very large crystallites are formed where the grain boundaries sweep in a second over micrometers. Again, in principle, only crystals with the (0001) plane parallel to the surface develop. Voids tend to be pushed to the "tilt boundaries" between these grains.

IV. DISCUSSION

Crystallization (with the sample holder at room temperature) of amorphous $Ge_2Sb_2Te_5$ under the electron beam of a TEM was mentioned in Ref. 14. Working at 200 kV acceleration voltage instead of the normal 400 kV (and defocusing the beam on the specimen) removed their problems with crystallization of 80 nm thick $Ge_2Sb_2Te_5$. In the present work, we did not observe crystallization under a 200 kV
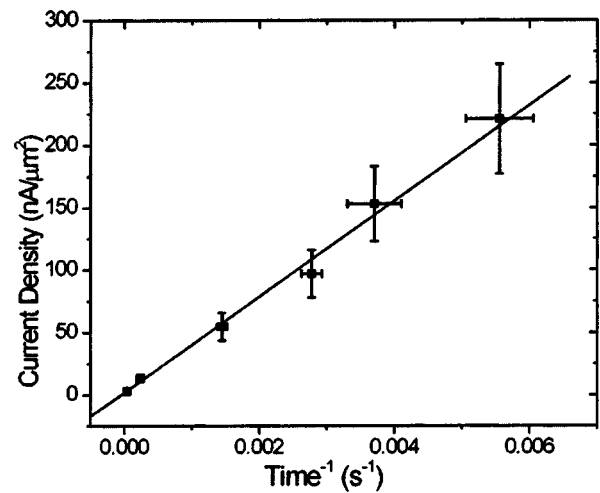

FIG. 9. The reciprocal of the incubation time for crystallization of a 40 nm thick $Ge_2Sb_2Te_5$ film as a function of the current density of a 400 kV electron beam going through the film (with the sample holder at room temperature) shows that they can be linearly related.

electron beam with the sample holder at room temperature. However, at 70 °C, we could invoke crystallization after 5–10 min under the electron beam for all three film thicknesses investigated (10, 40, and 70 nm). Most likely, crystallization is possible at lower temperatures, but then a longer incubation time holds for crystallization. We used a field-emission gun TEM, where high current densities can be attained, because the current can be confined into small probe sizes. However, the total current in the probe that is going through the specimen is generally much less than produced by a LaB_6 filament. Our JEOL 2010F was operated at a probe current of about 3 nA, whereas we operate the JEOL 4000 EX/II generally with a (relative low) probe current through the sample of the order of 30 nA. We tested if we could crystallize a 40 nm thick film with the holder at room temperature using this 400 keV 30 nA current. Indeed, this turned out to be possible.

Measuring the incubation time for crystallization as a function of current density of the electron beam led to the results presented in Fig. 9. When the current density I (in $nA/\mu m^2$) is plotted versus the reciprocal of the incubation time t_i (in. s^{-1}), the results can be fitted quite well by

$$I = (3.94 \pm 0.16)10^4 \frac{1}{t_i} + (0.17 \pm 4.8).$$

According to our expectation, an infinitely high current density is needed for $t_i = 0$. However, a priori we did not expect that for a current density going to zero, the incubation time would go to infinity. Therefore, we did not force the fit to go through $I = 0$ for $1/t_i = 0$, but the resulting value $I = 0.17 \pm 4.8$ shows that it effectively holds. This finding is important, because it indicates that there is no finite current density below which the incubation time goes to infinity. Thus even for the lowest dose, an effect of the electron beam on the crystallization process is expected. One can argue that if the incubation time is long enough (e.g., more than 10 h), the effect of the corresponding electron beam on the crystallization process will be negligibly small (because at higher tem-

peratures, the kinetics are such that crystallization occurs within minutes). However, this reasoning is incorrect. In Fig. 3, we see that a 200 kV beam with a diameter of 5.4 μm clearly altered the kinetics and morphology of crystallization. The current density in this case was only 0.12 nA/μm^2. If we insert this value in the above equation, the incubation time would be about 100 h at room temperature for a 400 kV electron beam and even longer for a 200 kV one. Still, the effect in Fig. 3 is substantial. Hence, the conclusion is that it appears impossible to avoid the influence of the electron beam on the crystallization of Ge$_2$Sb$_2$Te$_5$.

Defocusing the beam even more strongly using very small current densities may still be used to minimize (although not totally avoiding) the influence of the electron beam on the crystallization process. Then, the question is if the signal-to-noise ratio still allows fast capturing (e.g., on video tape) of images during crystallization that are clearly interpretable. Based on the present discussion, it is quite remarkable that the kinetic study performed in Ref. 15 by *in situ* TEM using a JEOL 4000 EX operating at 400 kV and capturing images with 25 frames/s did not suffer from the influence of the electron beam on the crystallization process.

Generally, a higher accelerating voltage reduces specimen heating and radiolysis by the electron beam, but increases displacement damage by knock-on collisions.[24] The present results and the ones reported in Ref. 14 show that at 400 kV crystallization is more promoted than at 200 kV. This clearly indicates that the effect of the electron beam is displacement damage and not radiolysis or specimen heating. Also, the difference in crystallization morphology inside and outside the area irradiated (cf. Fig. 3) indicates that the influence of the electron beam is not a simple heating effect. Then, the same morphology as observed at 130 °C would have been observed at lower temperatures under the electron beam, which is not the case.

The relation between the threshold displacement energy E_d of atoms and the required electron irradiation energy E_0 is:[25]

$$E_d = \frac{2E_0(E_0 + 2m_0 c^2)}{M c^2},$$

where m_0 is the electron rest mass, c is the speed of light, and M is the atomic mass of the target atom (all in Systeme International units). If no displacements are observed for a 200 keV beam, then the threshold displacement energies of Ge, Sb, and Te are larger than 7.2, 4.3, and 4.1 eV, respectively. If these atoms are displaced for $E_0 = 400$ keV, then E_d is equal or smaller than 17, 10, and 9.6 eV for Ge, Sb, and Te, respectively. It is not clear if crystallization requires that all three kinds of atoms are displaced. Maybe the displacement of one or two kinds of atoms and the accompanying production of free volume (here, we do not speak of, e.g., vacancies in the starting amorphous structure) is sufficient to largely increase the probability that a nucleus with a size equal to or larger than the critical one is formed (at the actual temperature). At least Ge has to be displaced, implying that its displacement energy is equal to or smaller than 17 eV and larger than 7.2 eV. This value is reasonable since the typical

range for E_d is from 5–50 eV (Refs. 24 and 25) and we expect that the bonding between the atoms are not so strong in this relatively soft amorphous alloy.

The large colonies outside the electron-irradiated area (cf. Fig. 3) indicate that nucleation is the rate-limiting step and that once a stable nucleus is formed, colonies can grow relatively fast. In contrast, small randomly oriented grains are present inside the irradiated area. Apparently, the excitations by the energetic electrons clearly facilitate the formation of stable nuclei. Because so many nuclei are initially formed simultaneously, their growth is spatially limited due to the neighboring nuclei. A second possibility is that the growth of the crystallites is hampered by the electron irradiation and, in this way, the nuclei are formed sequentially over a larger time span, but that it still results in a crystallized film with only small randomly oriented grains. The present work on Ge$_2$Sb$_2$Te$_5$ does not allow discrimination between these two possibilities. However, a subsequent *in situ* TEM crystallization study of fast growth Sb-rich phase change material (instead of the present fast-nucleation material) revealed that growth speeds are not affected by the electron irradiation, only the nucleation rate, in particular for the low temperatures near T_C. Although the materials are different, it is likely that also in Ge$_2$Sb$_2$Te$_5$ growth is unaffected by the electron irradiation.

It has been shown that the crystallization of Ge$_2$Sb$_2$Te$_5$ is nucleation driven (growth limited).[4] On the other hand, crystallization of Ag–In–Sb–Te (Ref. 4) or doped eutectic Sb$_2$Te Ref. 26 is growth driven. The observation of large colonies at 130 °C in the present experiments on Ge$_2$Sb$_2$Te$_5$ seems to contradict that growth is the rate-limiting step. Several factors can explain the discrepancy. The experiments for proofing the nucleation-driven crystallization of Ge$_2$Sb$_2$Te$_5$ were performed in real disk structures, where the adjacent dielectric layers may have promoted nucleation. However, the same experiments and some others[15,27] indicated that the nucleation rate is reduced at the GeSbTe–ZnS/SiO$_2$ interface. So, this cannot be the explanation. On the other hand, it is likely that at 130 °C, the amount of superheating is too small for a sufficient number of nuclei to form. In accordance with classical nucleation theory, a slight increase in temperature results in an explosive increase in the number of stable nuclei. This increase is much stronger than the accompanying increase in growth rate. So, only in a small temperature interval, just above the critical temperature for crystallization, large colonies can develop. Therefore, in most experiments, using laser and thermal heating at higher temperatures (say from 150 °C and higher), with more superheating, the large colonies will be absent. The present observations are not anomalous, because any phase transformation will show a temperature interval close to the one where the two phases are in equilibrium where the transformation is nucleation limited.

The typical bending-contour contrast of the spherulites, as we observed with TEM (cf. Figs. 3 and 5), was also observed, but not identified and recognized as such in the doped eutectic Sb$_2$Te phase change material.[26] Due to its growth-driven crystallization, this material will, in general, show this typical bending-contour contrast, whereas

$Ge_2Sb_2Te_5$ will only show it just above the crystallization temperature.

The observation (using the spherulites) that crystal nucleation starts at the lowest temperature at the film/vacuum interface and not at the film/Si-nitride interface agrees well with the results obtained by Ohshima[27] that the crystallization temperature of a single $Ge_2Sb_2Te_5$ layer is 15 K lower than when this film is sandwiched between Si_3N_4 films. Moreover, using cross-sectional TEM nucleation was directly observed to occur at the surface instead of at the interface with an Si substrate.[5] Although Fig. 4 shows which cap of a sphere or ellipsoid corresponds to the actual observations; these caps should not be interpreted as the growth fronts of the spherulites. In fact, we did not really demonstrate that nucleation occurs at the film/vacuum interface, but we established that the bending within the colony is such that the center of the spherulite is at the vacuum side as shown in Fig. 4. The most logical growth mode of a colony is that after nucleation, with a $\langle 111 \rangle$ axis perpendicular to the surface, growth is fastest along this axis across the whole thickness of the film. During this perpendicular growth, the $\langle 111 \rangle$ axis may already show a divergence when it approaches the Si-nitride. During the (subsequent) lateral growth, the $\langle 111 \rangle$ axis slowly, but continuously, tilts from the perpendicular direction to the in-plane direction. Although it is tentative, the driving force for this growth mode is possibly the competition between the surface energy (that favors $\langle 111 \rangle$ perpendicular to the surface) and the fastest growth direction that favors a $\langle 111 \rangle$ direction in the plane of the film (requiring a maximum tilt of 19.5° within a colony due to the presence of the other equivalent $\langle 111 \rangle$ directions). More detailed work is needed to unravel the actual growth mechanism of these crystalline $Ge_2Sb_2Te_5$ colonies.

V. CONCLUSIONS

The crystallization of amorphous $Ge_2Sb_2Te_5$ films (10, 40, and 70 nm thick) was studied by *in situ* heating in a transmission electron microscope. In a temperature interval between 70 and 125 °C, crystallization only occurred when aided by the 200 kV electron beam. Using a 400 keV beam, crystallization was possible with the sample holder at room temperature. The reciprocal of the incubation time for crystallization turned out to scale linearly with the current density of the 400 keV beam. It was demonstrated that, in principle, the electron beam always affects the crystallization process. Nucleation is strongly promoted by the electron beam and observations suggest that crystal growth remains unaffected. The main effect of the electron irradiation is displacement damage by knock-on collisions and not radiolysis or specimen heating.

At a temperature of 130 °C and higher, crystallization also occurs without electron irradiation. Just above the critical temperature for crystallization large colonies (typical size 400 nm) of 10–20 nm crystallites develop showing typical high symmetry bending contour contrast. These colonies can be identified as thin top sections (a cap) of spherulites. They developed in the 40 and 70 nm thick films, but not in the 10 nm ones. Most abundant are spherulites with a $\langle 111 \rangle$ zone

axis of the NaCl-type $Ge_2Sb_2Te_5$ structure perpendicular to the surface. Careful analysis shows that nucleation starts at the film/vacuum and not at the film/Si-nitride interface. At higher temperatures, crystals in the spherulites coarsen and their mutual orientation relation is gradually lost and also voids develop in the film.

At a temperature of 340 °C, the transformation to the stable trigonal crystal structure ($P\bar{3}m1$) of $Ge_2Sb_2Te_5$ occurs. The transition is characterized by very fast and excessive grain growth with the [0001] axis of the grains perpendicular to the surface. It is also shown that oxidation of the film strongly affects its crystallization; the critical temperature for crystallization lowers from 130 to 35 °C. Even at this low temperature, crystallization is a very fast process. Removal of Ge by its preferential oxidation is held responsible for the change in the crystallization process.

ACKNOWLEDGMENT

[1] N. Yamada, E. Ohno, K. Nishiuchi, and N. Akahira, Jpn. J. Appl. Phys., Suppl. **26**, 61 (1987).

[2] K. Nishimura, M. Suzuki, I. Morimoto, and K. Mori, Jpn. J. Appl. Phys., Suppl. **28**, 135 (1989).

[3] H. J. Borg and R. van Woudenberg, J. Magn. Magn. Mater. **193**, 519 (1999).

[4] G.-F. Zhou, Mater. Sci. Eng., A **304**, 73 (2001).

[5] T. H. Jeong, M. R. Kim, H. Seo, S. J. Kim, and S. Y. Kim, J. Appl. Phys. **86**, 774 (1999).

[6] I. Friedrich, V. Weidenhof, W. Njoroge, P. Franz, and M. Wuttig, J. Appl. Phys. **87**, 4130 (2000).

[7] V. Weidenhof, N. Pirich, I. Friedrich, S. Ziegler, and M. Wuttig, J. Appl. Phys. **88**, 657 (2000).

[8] V. Weidenhof, I. Friedrich, S. Ziegler, and M. Wuttig, J. Appl. Phys. **89**, 3168 (2001).

[9] P. K. Khulbe, E. M. Wright, and M. Mansuripur, J. Appl. Phys. **88**, 3926 (2000).

[10] T. Nonaka, G. Ohbayashi, Y. Toriumi, Y. Mori, and H. Hashimoto, Thin Solid Films **370**, 258 (2000).

[11] N. Yamada and T. Matsunaga, J. Appl. Phys. **88**, 7020 (2000).

[12] N. Nobokuni, M. Takashima, T. Ohno, and M. Horie, J. Appl. Phys. **78**, 6980 (1995).

[13] F. Jiang, Y. Xu, M. Jiang, and F. Gan, J. Non-Cryst. Solids **184**, 51 (1995).

[14] I. Friedrich, V. Weidenhof, S. Lenk, and M. Wuttig, Thin Solid Films **389** , 239 (2001).

[15] G. Ruitenberg, A. K. Petford-Long, and R. C. Doole, J. Appl. Phys. **92**, 3116 (2002).

[16] T. J. Kono and R. Sinclair, Mater. Sci. Eng., A **179**, 297 (1994); Acta Metall. Mater. **42**, 1231 (1994).

[17] V. Weidenhof, I. Friedrich, S. Ziegler, and M. Wuttig, J. Appl. Phys. **86**, 5879 (1999).

[18] B. J. Kooi and J. T. M. De Hosson, J. Appl. Phys. **92**, 3584 (2002); Note that twice (in the caption of Fig. 1 and in Sec. V, erroneously the value 1.827 nm is given for the *c*-lattice constant instead of the correct value 1.727 nm.

[19] A. K. Petford-Long, R. C. Doole, C. N. Alfonso, and J. Solis, J. Appl. Phys. **77**, 607 (1995).

[20] J. Vrijmoeth, H. A. van der Vegt, J. A. Meyer, E. Vlieg, and R. J. Behm, Phys. Rev. Lett. **72**, 3843 (1994); H. A. van der Vegt *et al.*, Surf. Sci. **365**, 205 (1996); H. A. van der Vegt *et al.*, Phys. Rev. B **57**, 4127 (1998).

[21] M. Chen, K. A. Rubin, and R. W. Barton, Appl. Phys. Lett. **49**, 502 (1986).

[22] E. Morales-Sanchez, E. Prokhorov, Y. Vorobiev, and J. Gonzalez-Hernandez, Solid State Commun. **122**, 185 (2002).

[23] M. H. R. Lankhorst, J. Non-Cryst. Solids **297**, 210 (2002).

[24] D. B. Williams and C. B. Carter, *Transmission Electron Microscopy* (Plenum, New York, 1996), Vol. I, pp. 61–65.

[25] L. W. Hobbs, *Introduction to Analytical Electron Microscopy*, edited by J. J. Hren, J. I. Goldstein, and D. C. Joy (Plenum, New York, 1979), p. 437.

[26] H. Borg, M. Lankhorst, E. Meinders, and W. Leibrandt, Mater. Res. Soc. Symp. Proc. **674**, V1.2.1 (2001); H. J. Borg, M. van Schijndel, J. C. N. Rijpers, M. H. R. Lankhorst, G. Zhou, M. J. Dekker, I. P. D. Ubbens, and M. Kuijper, Jpn. J. Appl. Phys., Part 1 **40**, 1592 (2001).

[27] N. Ohshima, J. Appl. Phys. **79**, 8357 (1996).